

A MULTI-SCALE APPROACH TO PREDICT THE IMPACT RESISTANCE OF BRAIDED COMPOSITES USING PROGRESSIVE FAILURE

Xu Lei, Khazar Hayat *, Sung Kyu Ha

Dept. of Mech. Eng., Hanyang University, 1271, Sa 3-dong, Sangnok-gu, Ansan, Kyeonggi-do, 426-791, Republic of Korea

*Author to whom correspondence should be addressed: email: khazarhayat@gmail.com

Received 29 June 2016; accepted 28 November 2016

ABSTRACT

A novel multi-scale approach based on micromechanics of failure together with the progressive damage models of the fibre and matrix constituents is presented to predict the impact resistance of braided composites. The meso- and micro-scale unit-cells of the braided composites with both thermosetting and thermos-plastic resin systems, were employed, and the effective properties of the braided tows, in the meso unit cell, were updated using the micro unit cell for which the degradation of constituent material properties were incorporated.

Key words: Braided composites; Impact resistance; Micromechanics of failure; Progressive damage model

1. INTRODUCTION

Recently, a rapid growth of the applications of braided fabric reinforced composites have been observed due to its net-shape fabrication, resistance to delamination damage and impact load resistance in particular [1]. For the development of composite structures made of braided composites, the numerical simulations can play a key role in reducing time and cost. However, the behaviour of the braided composites is not fully understood yet, and there is a need of establishing a generic methodology that can predict the material failure behaviours of the braided composites, but also other kinds of textile fabric composites subjected various types of loadings, including the impact loading [2].

A multi-scale approach based on micromechanics of failure (MMF) theory [3] and using progressive damage models is proposed to investigate the impact resistance of impacted braided composites. The impact behaviour of bi-axial (BX) braided composites subjected to impact load with thermoplastic and thermosetting resin systems is then investigated. The BX braided composite is selected due to its light weight and simplicity in numerical modeling and analysis. Since, the proposed methodology is based fundamental constituents of composite materials, which are the fibre and matrix, therefore, once the mechanical properties of constituents are obtained, any type of composite structure can be analysed under various circumstances such as thermal and moist environments. Therefore, it has a wide range of applications, and can be applied to various kinds of textile fabric reinforced composites subjected to different types of loadings.

2. MICROMECHANICS-BASED PROGRESSIVE DAMAGE MODEL

2.1 Multi-scale analysis

Before multi-scale analysis, the development of an idealized model of the braided composites is necessary to pre-

dict their mechanical behaviour. The fibre bundle arrangements are modelled using the geometrical parameters (i.e. braiding angle, width and thickness of axial tow, width and thickness of bias tow, and gap between bias tows) illustrated in Fig. 1a. Moreover, the undulation of tows plays a pivotal role in determining the behaviour of the braided composites. Further details on modeling procedure and techniques can be found in [2].

The multi-scale analysis procedure involves three scopes: macro, meso and micro, as shown in Fig. 1b. A braided composite can be assumed to be limited to meso scale, and consists of tows and pure matrix encapsulating the tows. Thus, the use of meso scale unit cell model serves as a bridge for transformation of stresses and effective material properties between the macro-level and micro level analyses.

It should be noted that a braided composite tow can be approximated as a curved continuous unidirectional (UD) lamina, and a micro unit cell can be used to relate the behaviour of fibre and matrix constituents to the tow behaviour as shown in Fig. 1c. Consequently, the meso and micro level analyses are linked to characterize the material behaviour of the tows of the braided composites. The meso stresses of tow can be transformed into the micro stresses of each constituent, and resulting constituent damages can be used to determine the tow damage, and, finally, the impact behaviour of braided composite at the macro level can be predicted. For the constituent damage analysis, the degradation of the constituent stiffness properties is carried out, and the tow effective material properties are subsequently updated through the micro unit cell.

The transformation between the tows stresses at meso level, denoted by ($\bar{\sigma}$) and the fibre and matrix stresses at micro level, denoted by σ_f , and σ_m , is carried using the stress amplification factors (SAFs), denoted by **M** and **A**

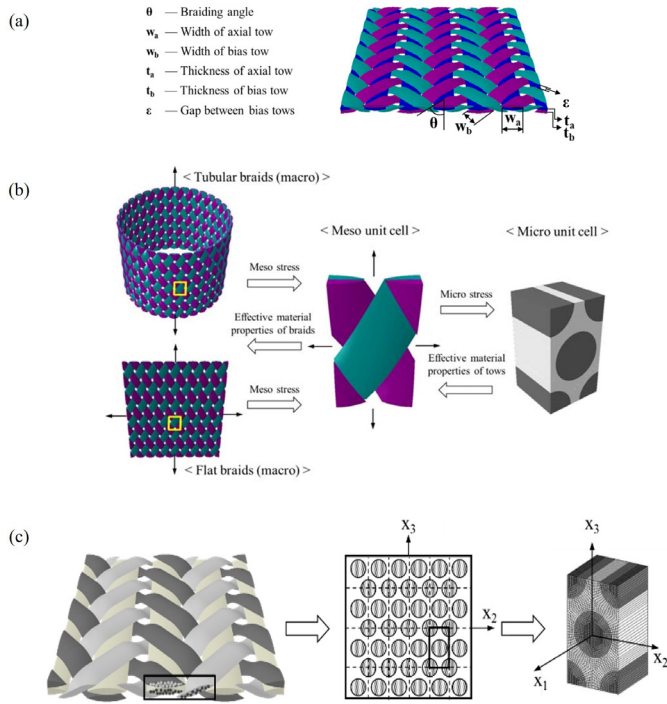


Fig. 1: (a) Geometry of braided composites, (b) multi-scale modelling approach, and (c) representation of braided tows as unit-cell model

matrices, as following [3, 4]:

$$\sigma_f = \mathbf{M}_f \bar{\sigma} + \mathbf{A}_f \Delta T$$

$$\sigma_m = \mathbf{M}_m \bar{\sigma} + \mathbf{A}_m \Delta T$$

In a similar manner, the meso strain and temperature increment can also be transformed to micro strains, as shown in Eq. 3, using the strain amplification factors which can be derived from SAFs using the constituent compliance matrix \mathbf{S} and the unit cell compliance matrix ($\bar{\mathbf{S}}$)

$$\mathbf{M}_s = \mathbf{S} \mathbf{M}_o \bar{\mathbf{S}}^{-1}, \mathbf{A}_s = \mathbf{S} \mathbf{A}_o$$

2.2 Damage model of micro constituents

For each constituent, a separate failure criterion is used due to their distinct mechanical behaviours. Considering the isotropic nature of the matrix constituent, the von-Mises failure criterion [3, 5] is used, which follows:

$$\frac{\sigma_{VM}^2}{C_m T_m} + \left(\frac{1}{T_m} - \frac{1}{C_m} \right) I_1 = 1$$

where I_1 , σ_{VM} , T_m , and C_m represents the first stress invariant, von-Mises equivalent stress, tensile strength and compressive strengths of matrix constituent, respectively. The failure criterion described by Eq. 3 matches the condition that the Stassi's equivalent stress σ_{eq} , reaches the matrix tensile strength T_m :

$$\sigma_{eq} = \frac{(\beta - 1)I_1 + \sqrt{(\beta - 1)^2 I_1^2 + 4\beta \sigma_{VM}^2}}{2\beta}$$

where the symbol β represents the ratio of the compressive strength to the tensile strength of the matrix constituent. Further, the equivalent stress can be transformed into the equivalent strain of the matrix constituent, described in Eq. 5, using the stress-strain relations.

$$\epsilon_{eq} = \frac{(\beta - 1)J_1 + \sqrt{(\beta - 1)^2 J_1^2 + \left(\frac{2 - 4\nu}{1 + \nu} \right)^2 \beta \epsilon_{VM}^2}}{2\beta(1 - 2\nu)} \quad (5)$$

where J_1 , ϵ_{VM} , and ν represents the first strain invariant, the von Mises equivalent strain and the Poisson's ratio of the matrix constituent.

It should be noted that the equivalent strain, like the equivalent stress, is a scalar quantity that is computed from the strain components. Fig. 2a represents a multi-linear stress-strain model defined using the equivalent stress and the equivalent strain, to estimate the matrix constituent damage. The matrix constituent behaves in a linear manner, before the occurring of any damage. Once damage occurs, the matrix constituent demonstrates a nonlinear behaviour (i.e. hardening followed by the softening depending on the damage status). The stiffness of the matrix constituent is degraded by a factor D_m as following:

$$D_m = 1 - \frac{(\epsilon_y^{(i)} - \epsilon_{eq}) \sigma_y^{(i-1)} + (\epsilon_{eq} - \epsilon_y^{(i-1)}) \sigma_y^{(i)}}{E_0 (\epsilon_y^{(i)} - \epsilon_y^{(i-1)}) \epsilon_{eq}} \quad (6)$$

subjected to the condition: $\epsilon_y^{(i)} \leq \epsilon_{eq} \leq \epsilon_y^{(i-1)}$. The symbols $\sigma_y^{(i-1)}$, $\epsilon_y^{(i-1)}$ denotes the matrix yield stress and the matrix yield strain at the beginning, and the symbols $\sigma_y^{(i)}$, $\epsilon_y^{(i)}$ denotes the matrix yield stress and matrix yield strain at the end of i th step. The symbol ϵ_{eq} denotes the current equivalent strain of the matrix at the i th step, and the symbol E_0 denotes the matrix intact stiffness.

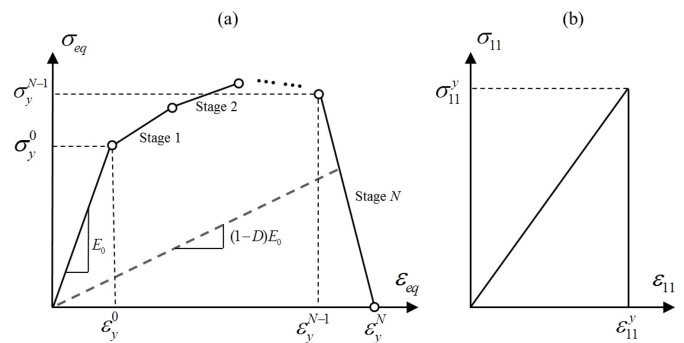


Fig. 2: (a) Multi-linear model for the matrix constituent damage, and (b) linear model for the fibre constituent damage

For the meso scale model, the damage in the pure matrix was modelled using Eq. 8 only, and additional MMF-based damage modeling using a micro unit cell was used for the matrix of tows [6]. The periodic boundary conditions were used for the meso and micro unit cells [2, 7]. The micro unit cell model, based on the MMF theory and linear material model, delivered multi-axial micro stress state for the fibre and the matrix constituents (i.e. assuming perfect

bonding for interface). To avoid computation instability, the maximum local damage value for fibre and matrix constituent was set to 0.9 [8].

The meso scale stresses $\bar{\sigma}$ were applied on the micro unit cell. After performing the finite element analysis, the micro stresses/strains in the matrix were computed. Afterwards, the damage analysis for the matrix was performed. For the matrix of tow, the localization of damage was avoided by using a volume-based damage homogenization technique, represented by Eq. 8 shown below:

$$\bar{D}_m = \frac{\int_0^V [D_m]^p dV}{\int_0^V dV} \quad (7)$$

where the symbol p denotes a positive weighing factor, and the symbol V denotes the matrix overall volume in the micro unit cell.

After estimation of damage status, the tow effective material properties in the meso unit cell model were re-evaluated from the micro unit cell and the matrix material properties were degraded. Afterwards, the damage propagation inside the tows and the pure matrix was evaluated. For the matrix constituent, following constitutive relation was used to degrade the stiffness:

$$\sigma_m = (1 - \bar{D}_m) C_m \epsilon_m \quad (8)$$

where C_m denotes the stiffness of matrix zone in the micro unit cell.

For the fibre constituent, the maximum stress failure criterion, which is $-C_f \leq \sigma_{f11} \leq T_f$, was used for the fiber constituent. The symbol σ_{f11} presents the micro longitudinal stress of the fibre constituent, and symbols T_f and C_f denotes the longitudinal tensile strength and longitudinal compressive strength of the fibre constituent, respectively. Fig. 2b illustrates that when the fibre constituent fails its stiffness is dramatically degraded. Since, carbon fibre behaves in a brittle manner, therefore, the highest value of all elemental damage factors was considered, as following:

$$\bar{D}_f = \max(D_f^{(j)}) \quad (9)$$

where the symbol $D_f^{(j)}$ denotes the damage factor of j th element of the fibre constituent. And, the constitutive relation for fibre constituent was:

$$\sigma_f = (1 - \bar{D}_f) C_f \epsilon_f \quad (10)$$

where C_f denotes the stiffness of overall fiber zone in the micro unit cell.

2.3 Numerical implementation

Fig. 3 illustrates the flow chart of the algorithm developed

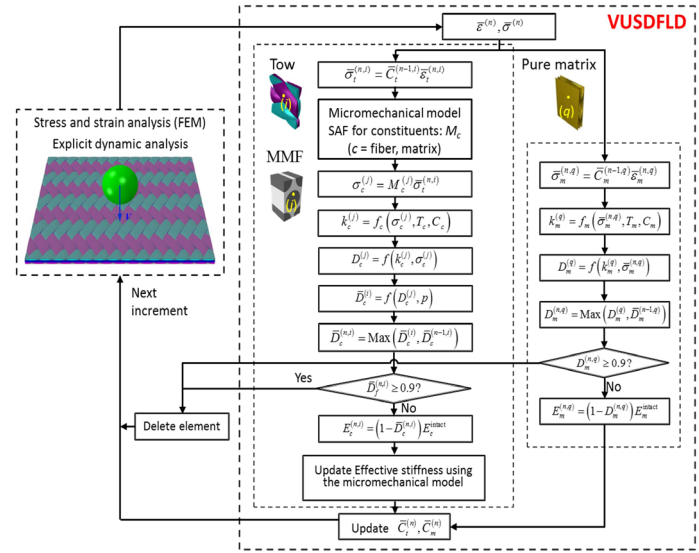


Fig. 3: Algorithm combining the MMF methodology and progressive damage models

for combining the MMF methodology and progressive damage model. In the beginning, the total global strain, denoted by $\bar{\epsilon}^{(n)}$, is computed at the global time n , and augmenting the global strain increment, denoted by $\Delta\bar{\epsilon}^{(n)}$ to global strain at previous time-step $n-1$. For the tows, the macro stresses of each tow element, denoted by $\bar{\sigma}_t^{(n,i)}$, are estimated using the previous effective stiffness properties, denoted by $\bar{C}_t^{(n-1,i)}$. Afterwards, the micro stresses for each element of the both matrix and fibre zones in the micro unit cell, denoted by $\sigma_m^{(j)}$, $\sigma_f^{(j)}$ are computed from the meso stress, denoted by $\bar{\sigma}_t^{(n,i)}$, by using SAFs. The constituent failure criteria are then applied to both matrix and fibre, and damage factor is estimated for each j th element in the matrix and fibre zones, denoted by $D_m^{(j)}$ and $D_f^{(j)}$, respectively, by employing the relevant constituent damage models. The overall damage factor for both matrix and fibre zones, denoted by \bar{D}_m and \bar{D}_f , are then evaluated based on their respective damage methods (i.e. the damage homogenization for the matrix constituent, and the maximum damage for fibre constituent, as discussed previously).

Based on the status of overall damage factor, the stiffness properties of the matrix and fibre are degraded, and the tow effective properties are evaluated for the next time increment. The numerical implementation was done using ABAQUS 6.11-1, a commercial finite element solver, combined with its user subroutine VUSDFLD [9].

3. IMPACT ANALYSIS OF BRAIDED COMPOSITES

For impact analysis, the whole model of carbon fibre biaxial braided fabric composites having a braided angle of 45 degrees, hereafter denoted with BX45, was composed of fibre, pure matrix, matrix in tows, and a ballistic projectile. For the geometrical modeling parameters, the tow width and the two thicknesses used were 3.01 mm and 0.5 mm, respectively. There was a gap of 0.002 mm between the bi-

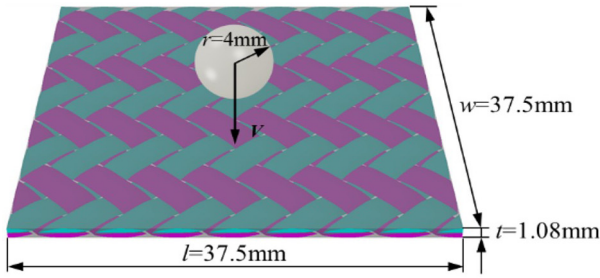


Fig. 4: Impact analysis of biaxial braided composites with braids at 45 degrees

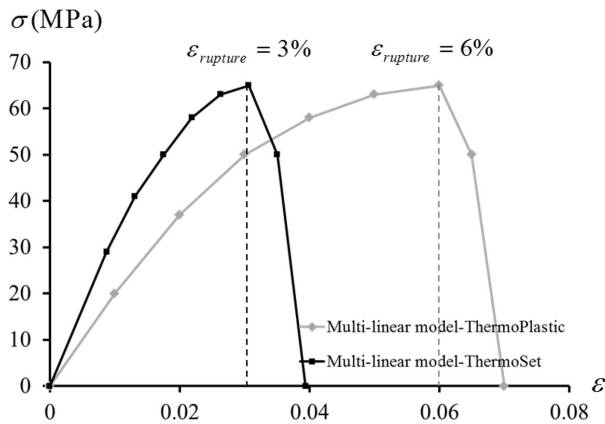


Fig. 5: Stress-strain behaviours of the matrix resin systems used tows. The amplitude of the tow undulation of biaxial braids was set to 0.252 mm.

Two kinds of BX45 composites with thermoplastic and thermosetting resin systems were investigated. The stiffness and strength properties of carbon fibre constituent are listed in Table 1 [1]. It should be noted that the strength properties of carbon fibres were back-calculated using micromechanics approach. The stiffness and strength properties of the matrix constituent, listed in Table 2, were taken from in-house material testing database. The tows effective properties, listed in Table 3, were computed from micro unit cell, using the stiffness properties of the matrix and fibre constituents, along with a fibre volume fraction of 0.78. It should be noted that the total fibre volume fraction of the meso unit cell was approximately 0.5, computed in accordance with [2]. The multi-linear damage models consisting of hardening and softening behaviours, shown in Fig. 5, for the matrix constituent (i.e. thermoplastic and thermosetting resin systems) was also established based on in-house test data.

For the ballistic projectile, the radius was 4 mm. The initial position of the projectile was set above the BX45 model and the gap between the bottom of the projectile and the top surface of the braided models was set to 0.1 mm. Fixed boundary conditions were applied on the all four sides of the braided composites, and the top and bottom boundaries of the braided model were assigned with free boundary conditions. The ballistic projectile was taken as a rigid body controlled by a reference point, which was

Table 1: Material properties of carbon fibres [1]

Material property	Value
Longitudinal modulus: E_{f1} (GPa)	276.0
Transverse modulus: E_{f2} (GPa)	27.6
In-plane shear modulus: G_{f12} (GPa)	138
Transverse modulus: G_{f23} (GPa)	7.8
Major Poisson's ratio: ν_{f12}	0.3
Major Poisson's ratio: ν_{f23}	0.8
Longitudinal tensile strength: T_f (MPa)	3800
Longitudinal compressive strength: C_f (MPa)	2980

Table 2: Material properties of the matrix resin

Material property	Thermosetting	Thermoplastic
Elastic modulus: E_m (GPa)	3.45	2
Elastic Poisson's ratio: ν_m	0.35	0.35
Final tensile strength: T_m (MPa)	65	65

Table 3: Tows effective material properties

Material property	Tows with thermosetting resin	Tows with thermoplastic resin
Longitudinal modulus: E_1 (GPa)	215.67	215.67
Transverse modulus: E_2 (GPa)	13.55	13.55
In-plane shear modulus: G_{12} (GPa)	9.0	9.0
Transverse modulus: G_{23} (GPa)	4.29	4.29
Major Poisson's ratio: ν_{12}	0.309	0.309
Major Poisson's ratio: ν_{23}	0.592	0.592

constrained to move only in z-direction. As illustrated in Fig. 4, the projectile was given an initial velocity, and the contact properties were also assigned on the braided model and the projectile by setting a value of 0.28 for the coefficient of friction. Once the projectile touches the top surface of the braided model, the contact behaviour will be taken into account. Two initial velocities of 20 m/s and 50 m/s were applied to the projectile. At initial velocity of 20 m/s, no penetration occurred and projectile bounced back after impact. However, at initial velocity of 50 m/s, the projectile penetrated through the braided composite.

4. RESULTS AND DISCUSSIONS

The impact resistance was qualitative evaluated by a visual inspection of the damage contours of the BX45 composite models with thermoplastic and thermosetting resins, subjected to the impact velocity 50 m/s as shown in Fig. 6. For the pure matrix and the matrix in tows, the damage contour with element deletion are shown in Fig. 6a-c and Fig. 6(b-d), respectively. Only the top-side of the damaged braided composite model, facing the incident projectile, is shown. Similar damage contours, along with element deletion, were also observed for the back-side of the braided

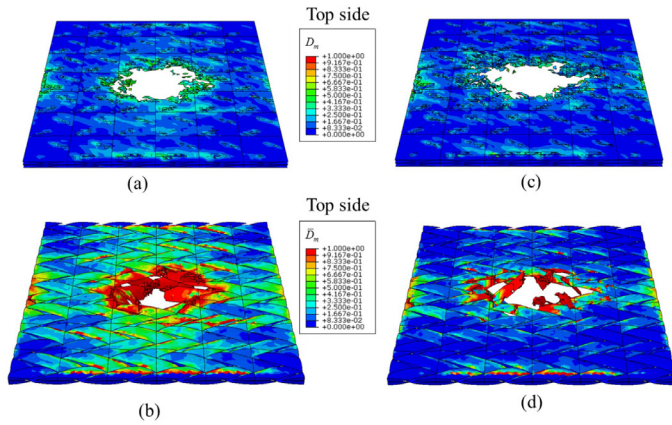


Fig. 6: Damaged matrix element deletion for BX45 braided composite at impact velocity of 50m/s: (a) pure thermoplastic matrix, (b) thermoplastic matrix in tows, (c) pure thermosetting matrix, and (d) thermoset resin in tows

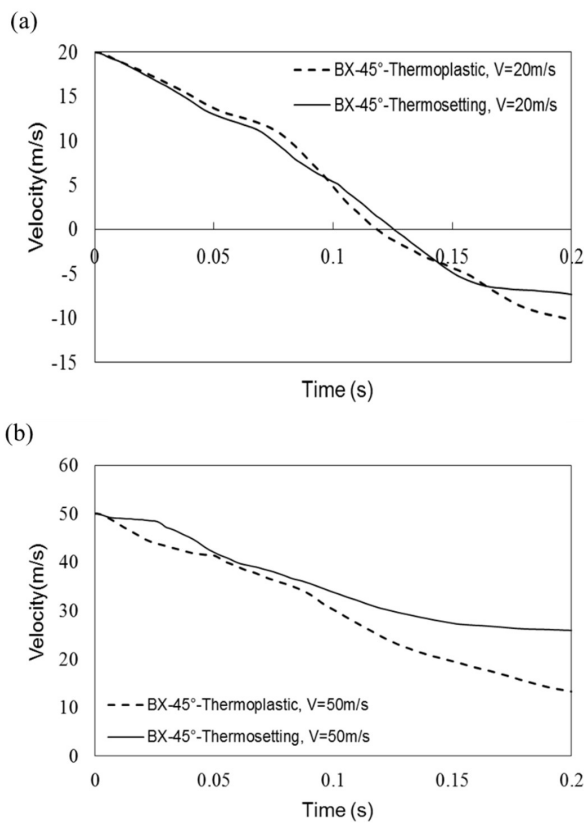


Fig. 7: Projectile velocity time histories for impact velocity of: (a) 20 m/s, and (b) 50 m/s

composite model. Based on the visual inspection of the damage contours, it can be qualitatively stated that the use of thermoplastic resin for the braided composite results in a better spreading of the impact energy, a lower damage area owing to lesser element deletion, and, consequently, improved impact resistance. Similar qualitative observations were made for braided composites subjected to a projectile with impact velocity of 20 m/s, and not shown for brevity.

In order to quantitatively study the impact resistance of BX45 braided composites, the evaluation of impact energy absorption in terms of a reduction in the projectile velocity

after impact, and the estimation of impact induced damage area in terms of the percentage element deletion was carried out. The projective velocity histories, after impact, for a duration of 0.2 seconds were recorded.

It should be noted that the projectile strikes the braided composites with an impact velocity and after the collision, the projectile bounces back with a rebound velocity if impact velocity is lower, otherwise, it penetrates through and possess a residual velocity. The reductions in rebound and residual velocities of the projectile, in a comparison to the incident impact velocity, demonstrate the impact energy absorption capacity of the braided composites. Fig. 7a shows that for BX45 braided composite model, the impact velocity of 20 m/s of the projectile decreases with the passage of time. The velocity becomes zero at the time between 0.1-0.15 seconds, and becomes negative afterwards, representing the rebounding of the projectile after impact. The recorded velocity histories for the braided composites both resin systems almost overlap, making it very difficult to differentiate their impact resistance behaviours at the impact velocity of 20 m/s. On the contrary, the impact resistance of the braided composite with thermoplastic and thermosetting resins, can be clearly distinguished at the projectile impact velocity of 50 m/s, as shown in Fig. 7b. The projectile penetrates through the braided composite at impact velocity of 50 m/s. The residual velocity of the projectile decreases with the passage of time, but remains positive throughout the recorded time of 0.2 seconds. For the BX45 braided composites, there was an approximately 49% reduction in the residual velocity, the thermosetting resin system was replaced with the thermoplastic resin. The reduction in residual velocity of the projectile means that the impact energy is absorbed by the braided composite model. Higher the decrease in the residual velocity of the projectile, the higher would be the impact energy absorption. Based on this fact, it can be inferred that the braided composite model with thermoplastic resin exhibits better impact resistance than that of the braided composite model with thermosetting resin.

The impact damaged areas were evaluated, in terms of a percentage element deletion, for the pure matrix and for

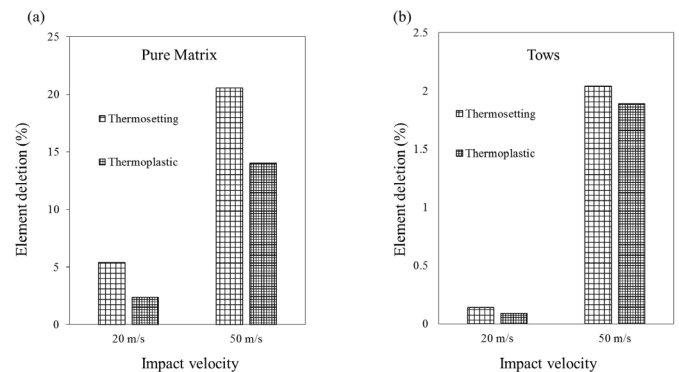


Fig. 8: Impact induced damage terms of element deletion for: (a) pure matrix, and (b) tows of the braided composites

the matrix in tows, respectively, of the BX45 braided composite, as shown in Fig. 8. For the pure resin, the percentage element deletion for the braided composite with thermosetting resin system was computed to be approximately 126% and 47% higher than that of the braided composite with thermoplastic resin system, for the incident impact velocities of 20 m/s and 50 m/s, respectively. Similarly, in the case of the matrix in tows, the percentage element deletion for the braided composite with thermosetting resin was approximately 56% and 8% higher than that of the braided composite with thermoplastic resin, for the incident impact velocities of 20 m/s and 50 m/s, respectively. The percentage of element deletion of the pure resin and of the matrix in tows for the braided composite with thermoplastic resin system is lower than that for the braided composite with thermosetting resin system, as it withstand higher impact loads. Since, the braided composite with thermoplastic resin system possess better impact resistance, therefore, the small number of elements reach the critical damage values that once reach results in the element deletion. Based on the evaluation of impact damaged areas in terms of percentage element deletion, it can be inferred that the braided composites with thermoplastic resin demonstrate better impact resistance than that of the braided composite model with thermosetting resin.

5. CONCLUSIONS

A multi-scale approach based on micromechanics of failure (MMF) together with the progressive damage models is demonstrated and applied to evaluate the impact resistance of biaxial braided composites with braiding angle of 45 degrees, made of thermoplastic and thermosetting resin systems. Two impact conditions, the bouncing back of projectile with an incident impact velocity of 20 m/s and the full perpetration of projectile at an incident impact velocity of 50 m/s, were simulated. The impact resistance were estimated based on the impact energy absorption in terms of the reduction in the impact velocity after impact, and computation of the impact damaged area in terms of the percentage of element deletion in the pure matrix and the matrix in tows. Results showed that the braided composites with thermoplastic resin demonstrate better impact resistance, than that of the braided composite with thermosetting resin, suggesting a need of selecting a suitable resin system to improve the impact resistance.

The proposed methodology is quite generic, as it begins with the fundamental constituents of composite materials (i.e. fibre and matrix), therefore, once the mechanical properties of constituents are obtained, any type of composite material and structure can be analysed under various circumstances such as thermal and moist environments. Therefore, it has the potential to cover a wide range of composite fabrics subjected to various types of loadings. Currently, the methodology is under extensive validation in the laboratory environment. Its validation results, along with various applications, will be reported in the near future.

References:

1. Sun, X.S. Tan, V.B.C. and Tay, T.E., "Micromechanics-based progressive failure analysis of fiber-reinforced composites with non-iterative element-failure method", *Computers and Structures*, **89** (2011), 1103-1116.
2. Xu, L. Kim, S.J. Ong, C.H. and Ha, S.K., "Prediction of material properties of biaxial and triaxial braided textile composites", *Journal of Composite Materials*, **46/18** (2012), 2255-2270.
3. Ha, S.K. Huang, Y. Han, H.H. and Jin, K.K., "Micro-mechanics of Failure for Ultimate Strength Predictions of Composite Laminates," *Journal of Composite Materials*, **44/20** (2010), 2347-2361.
4. Jin, K.K. Huang, Y. Lee, Y.H. and Ha, S.K., "Distribution of Micro Stresses and Interfacial Tensions in Unidirectional Composites", *Journal of Composite Materials*, **42/18** (2008), 1825-1849.
5. Raghava, R. Caddell, R.M. and Yeh, G.S.Y., "The macroscopic yield behaviour of polymers", *Journal of Materials Science*, **8/2** (1973) 225-232.
6. Fish, J. and Q. Yu., "Two-scale damage modeling of brittle composites", *Composites Science and Technology*, **61/15** (2001) 2215-2222.
7. Xia, Z. Zhang, Y. and Ellyin, F., "A Unified Periodical Boundary Conditions for Representative Volume Elements of Composites and Applications", *International Journal of Solids and Structures*, **40/8** (2003) 1907-1921.
8. Hashimoto, M. Okabe, T. Sasayama, T. Matsutani, H. and Nishikawa, M., "Prediction of tensile strength of discontinuous carbon fiber/polypropylene composite with fiber orientation distribution", *Composites Part A: Applied Science and Manufacturing*, **43/10** (2012) 1791-1799.
9. Roget, B. and Chopra, I., "Wind-tunnel testing of rotor with individually controlled trailing-edge flaps for vibration reduction", *Journal of Aircraft*. **45/3** (2008) 868-879.